Available online at www.sciencedirect.com
ScienceDirect
J. Mater. Sci. Technol., 2011, **27**(12), 1157-1164.
JMST
www.JMST.org

Effect of Rotation Rate on Microstructures and Mechanical Properties of FSW Mg–Zn–Y–Zr Alloy Joints

G.M. Xie[1)†], *Z.Y. Ma*[2)], *Z.A. Luo*[1)], *P. Xue*[2)] *and G.D. Wang*[1)]

1) The State Key Laboratory of Rolling and Automation, Northeastern University, Shenyang 110819, China

2) Shenyang National Laboratory for Materials Science, Institute of Metal Research, Chinese Academy of Sciences, Shenyang 110016, China

[Manuscript received June 7, 2011, in revised form June 29, 2011]

Friction stir welding (FSW) of Mg–Zn–Y–Zr plates with 6 mm in thickness was successfully carried out under a wide range of rotation rates of 600–1200 r/min with a constant traverse speed of 100 mm/min. After FSW, the coarse grains in the parent material (PM) were changed into fine equiaxed recrystallized grains at the nugget zone (NZ). Furthermore, the coarse Mg–Zn–Y particles (W-phase) were broken up and dispersed homogenously into the Mg matrix. With increasing rotation rates, the size of the W-phase particles at the NZ significantly decreased, but the recrystallized grain size tended to increase. The hardness values of the NZs for all the FSW joints were higher than those of the PM, and the lowest hardness values were detected in the heat affected zone (HAZ). The fracture occurred in the thermo-mechanical affected zone (TMAZ) on the advancing side for all the FSW joints in the tensile test, due to the incompatibility of the plastic deformation between the NZ and TMAZ caused by remarkably different orientation of grains and W-phase particles. The strength of FSW joint reaches 90% of that of its PM.

KEY WORDS: Friction stir welding; Magnesium alloys; Microstructure; Mechanical property

1. Introduction

Magnesium alloys exhibit lower density, higher specific strength, and good damping capacity than aluminum alloys[1,2]. Therefore, they are widely applied as structural parts in space probes and cars. To achieve high strength, the magnesium alloys must undergo thermo-mechanical processing (TMP), yielding a fine-grained microstructure. The conventional AZ (Mg–Al–Zn) series magnesium alloys have poor thermal stability due to the lower dissolution temperature of $Mg_{17}Al_{12}$ phase. Therefore, the easier grain growth and cavitation formation are the major problems during the hot deformation, resulting in decreasing mechanical property. Mg–Zn–Y–Zr alloys containing ternary phases (Mg_3Zn_6Y and $Mg_3Zn_3Y_2$) exhibited excellent mechanical properties at room temperature as well as at elevated temperature, because ternary phases with high thermal stability pinned the boundaries and inhibited grain growth during the TMP[3].

For the joints of the magnesium alloys produced by conventional fusion welding techniques, the welding defects such as porosity, crack and the excess eutectic are easily formed in the fusion zone. Friction stir welding (FSW), invented by The Welding Institute of the UK in 1991, is an energy-efficient, environment-friendly and versatile joining technique that has been proved to be one of the most remarkable achievements in the field of joining aluminum and magnesium alloys[4–7]. However, few slip systems operate in the close-packed hexagonal structure of magnesium alloys during plastic processing. Therefore, it is more difficult to obtain sound FSW joint of magnesium alloys than that of the aluminum alloys at a wide range of welding parameters.

In the past few years, a number of studies have been conducted to evaluate the feasibility of FSW of magnesium alloys. From the investigations on FSW of AZ (Mg–Al–Zn), AM (Mg–Al–Mn) and ZK (Mg–Zn–

† Corresponding author. Ph.D.; Tel.: +86 24 83673172; E-mail address: xiegm@ral.neu.edu.cn (G.M. Xie).

Table 1 Summary of friction stir welding condition for butt-joints

Tool description	Tool rotation rate/(r/min)	Tool traverse speed/(mm/min)
Shoulder diameter, 20 mm Pin length, 5.7 mm Threaded pin root diameter, 6 mm Pin tilt angle, 2.5 deg.	600, 800, 1200	100

Zr) series magnesium alloys, it was seen that sound FSW joints with uniform microstructure and good properties could be achieved only under optimized FSW parameters[8–17]. At present, however, only few investigations were conducted on the weldability of Mg–Zn–Y–Zr alloys by FSW. In our previous study[18], the microstructure and mechanical properties of FSW Mg–6.0Zn–0.6Y–0.6Zr alloy were investigated and the defect-free FSW joint could be successfully achieved at the selected tool rotation rate of 800 r/min and traverse speed of 100 mm/min. Furthermore, a comparison has been made between FSW joints of Mg–6.0Zn–0.6Y–0.6Zr and Mg–6.0Zn–0.6Zr alloys to evaluate the effect of Y addition[19]. Because the FSW of Mg–6.0Zn–0.6Y–0.6Zr was only conducted at one constant welding parameter of 800 r/min and 100 mm/min, it is worthwhile to further evaluate the weldability of Mg–Zn–Y–Zr alloys by FSW and the effect of FSW parameter on the mechanical properties of the joints.

In this paper, the rolled Mg–Zn–Y–Zr plate containing W-phase ($Mg_3Zn_3Y_2$) was subjected to FSW at wide tool rotation rates of 600–1200 r/min with a constant traverse speed of 100 mm/min. The purposes of this work are to obtain the optimum FSW parameter for the Mg–Zn–Y–Zr alloys and to establish the relationship between the microstructure and the mechanical properties of the joints.

2. Experimental

Mg–Zn–Y–Zr alloy plate with a composition of 7.1Zn–1.2Y–0.8Zr (in wt%) was used in this study. The rolled plates with 6 mm in thickness, 300 mm in length and 70 mm in width were butt-welded using a gantry FSW machine (China FSW Center). Table 1 shows a summary of FSW condition. Before welding, the plates were cleared by the wire brush to remove the surface oxide layer.

The FSW samples were cross-sectionally machined perpendicular to the welding direction, polished and then etched with a solution of 90 ml ethanol, 10 ml distilled water, 5 ml acetic acid and 5 g picric acid. Microstructural features were characterized by optical microscopy (OM, LEICA Q55OW, Germany) and scanning electron microscopy (SEM, FEI Quanta600, Japan). Grain sizes were measured by the mean linear intercept method. Distribution of element and composition of phase were analyzed by electron probe microanalysis (EPMA, JEOL-8530, Japan) and X-ray diffraction (XRD, Philips, PW3040160, Holand), respectively.

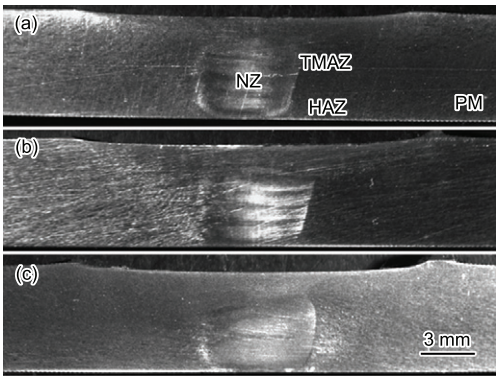

Fig. 1 Cross-sectional macrographs of FSW Mg–Zn–Y–Zr joints at 600 (a), 800 (b), and 1200 r/min (c) (traverse speed: 100 mm/min; the advancing side is on the right)

The Vickers microhardness tests of the joints were performed on the cross-section perpendicular to the welding direction using a LECO-LM247AT Vickers-hardness machine with 200 g load for 13 s. The transverse tensile specimens with a gauge length of 40 mm and a gauge width of 10 mm were machined perpendicular to the FSW direction. The tensile tests were carried out using a Zwick-Roell testing machine at a strain rate of 4.2×10^{-4} s^{-1}.

3. Results and Discussion

The typical cross-sectional macrographs of the FSW Mg–Zn–Y–Zr joints under different rotation rates are presented in Fig. 1. Defect-free welds are achieved under a wide rotation rate range of 600 to 1200 r/min at a constant traverse speed of 100 mm/min. Four distinct zones, namely parent material (PM), nugget zone (NZ), thermo-mechanically affected zone (TMAZ), and heat affected zone (HAZ), are identified in the FSW joints, as schematically shown in Fig. 1(a). Similar macrographs are obtained in the NZ at different rotation rates. The width of the NZ is about 6.1, 6.2 and 6.4 mm for 600, 800 and 1200 r/min, respectively. The width of the NZ is slightly enlarged with increasing rotation rate. Similarly, Gharacheh *et al.*[10] indicated that with increasing rotation rate, the width of the NZ of FSW AZ31 increased. In the previous work[16], a narrow NZ in FSW ZK60 alloy at a relatively low heat input was identified. It is well known that the heat input and plastic deformation during the FSW process could be

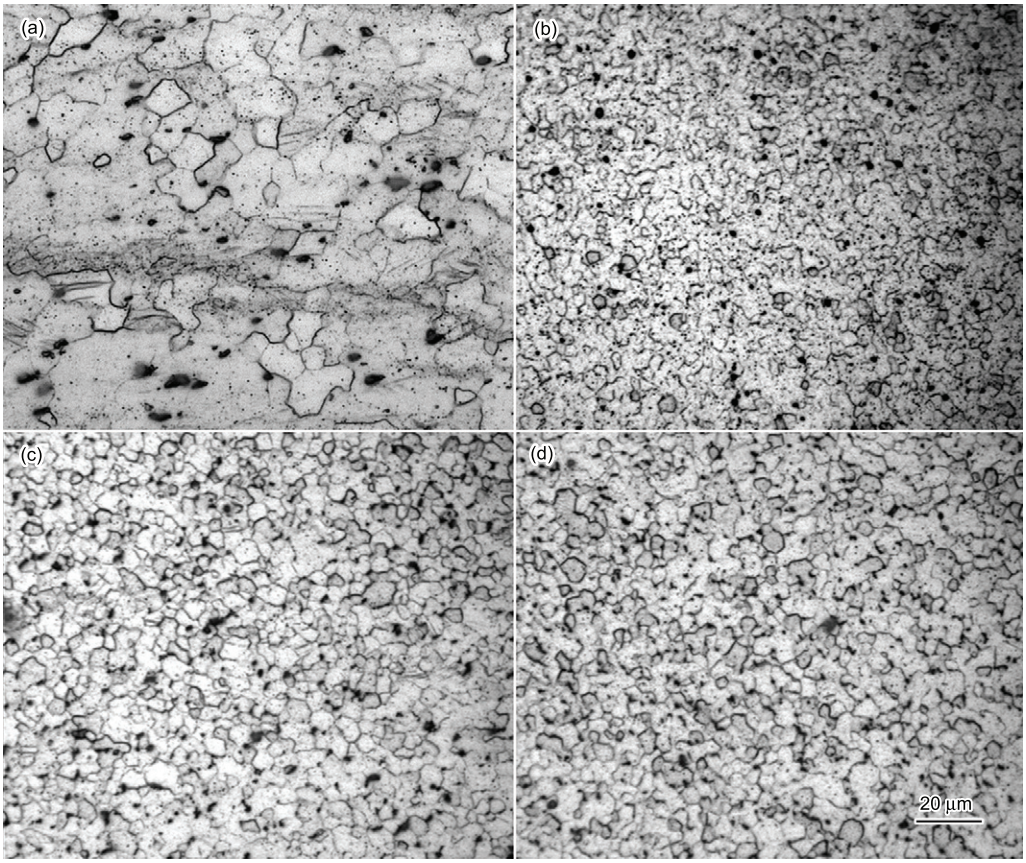

Fig. 2 Microstructures of PM (a) and NZ of FSW Mg–Zn–Y–Zr joints at 600 (b), 800 (c) and 1200 r/min (d) with a traverse speed of 100 mm/min

enhanced by increasing the rotation rate, promoting the material flow in the plastic deformation zone, *i.e.* the NZ. Therefore, the widest NZ was observed in the FSW Mg–Zn–Y–Zr joint at 1200 r/min in this study.

Figure 2 shows the microstructures of the PM and NZs under different rotation rates. The average grain size of PM and NZ at 400, 800 and 1200 r/min is 22, 3.2, 4.1 and 4.6 μm, respectively. The PM consists of inhomogeneous coarse grains and a certain amount of coarse secondary phase particles (Fig. 2(a)). Compared to the PM, the microstructures of the NZs are characterized by the fine and equiaxed recrystallized grains (Fig. 2(b)–(d)). In the NZ, the intense plastic deformation and thermal exposure result in the occurrence of dynamic recrystallization (DRX), thereby producing the remarkable microstructural refinement. Figure 2(b)–(d) indicate that the difference between the grain sizes of the NZ at different rotation rates is relatively small in the FSW Mg–Zn–Y–Zr alloy. The grain size in the NZ slightly increases as the rotation rate increases from 600 to 800 r/min, but the grain sizes in the NZ are quite similar at the rotation rates of 800 and 1200 r/min. By contraries, the grain size in the NZ of FSW ZK60 alloy obviously increased as the rotation rate increased from 800 to 1200 r/min with a constant traverse speed of 100 mm/min[16]. The heat input is determined by the rotation rates at a constant traverse speed in the FSW process. Compared to the ZK60 alloy, the Mg–Zn–Y–Zr alloy contains a great number of W-phase particles that would inhibit the growth of recrystallized grains. Therefore, the effect of the heat input on the microstructure in the NZ of FSW Mg–Zn–Y–Zr alloy is relatively limited.

Figure 3 shows the microstructures in the TMAZ of the FSW Mg–Zn–Y–Zr alloy at various rotation rates on the advancing side. The coarse elongated grains and strip-like second phase particles are distributed in the TMAZ along the outline of the NZ. This implies that DRX does not occur in the TMAZ of the present FSW Mg–Zn–Y–Zr alloy due to insufficient plastic deformation and thermal exposure. Similarly, the elongated grains appeared in the TMAZ of FSW Mg–Zn–Y–Zr alloy containing I-phase[18]. Besides, Zhang *et al.*[20] also found the elongated grains in the TMAZ of FSW Mg–Al–Ca alloy. For the conventional AZ series magnesium alloys, however, the DRX easily occurred in the FSW process due to the lower recrystallization temperature (∼523 K)[21], resulting in the complete dynamic recrystallization at the NZ and even at the TMAZ. Park *et al.*[11] reported that equiaxed recrystallized grains similar to those at the NZ were obtained at the TMAZ of FSW AZ61 alloy. Similarly, Yang *et al.*[8] also indicated that the grain sizes of NZ and TMAZ were much close in the

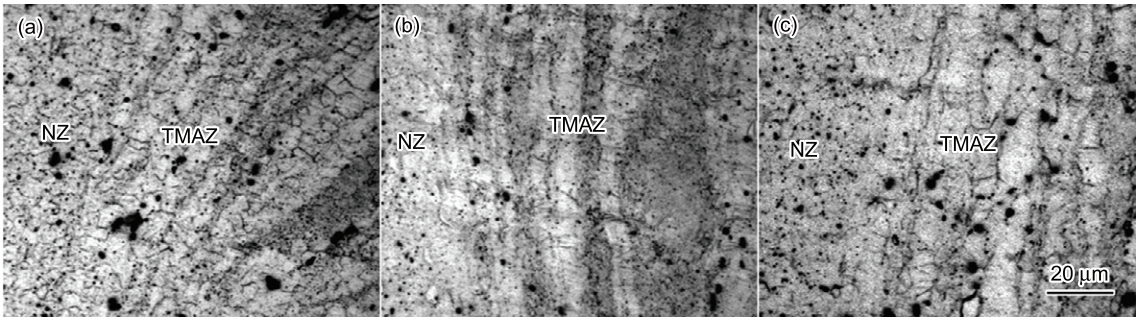

Fig. 3 Microstructures of TMAZ in advancing side of FSW joints at 600 (a), 800 (b) and 1200 r/min (c) with a traverse speed of 100 mm/min

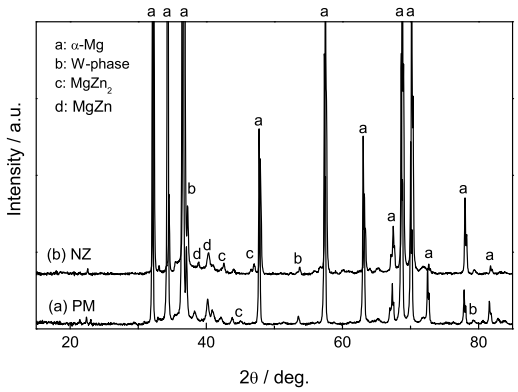

Fig. 4 X-ray diffraction pattern of Mg–Zn–Y–Zr alloy: (a) PM, (b) NZ (1200 r/min–100 mm/min)

weld of FSW AZ31 alloy. Therefore, a number of second phase particles in these heat-resistant magnesium alloys significantly inhibited the DRX in the TMAZ.

Figure 4 shows the XRD patterns of the PM and NZ at 1200 r/min. For the PM, the intense diffraction peaks of α-Mg and W-phase and the weak diffraction peaks of MgZn and $MgZn_2$ phases were detected, but no diffraction peak of the I-phase was found. After FSW, all diffraction peaks in the PM were remained, indicating that FSW did not cause the change of the second phases.

Figure 5 is the map distribution of Mg, Zn and Y elements in the PM and NZ at 1200 r/min by EPMA. It is indicated that most of the second phase particles in both PM and NZ should be the Mg–Zn–Y ternary phase, *i.e.* the W-phase according to the XRD results. A previous study[3] indicated that the W-phase with a high eutectic temperature of ~510°C had high thermal stability. Therefore, even under the high heat input condition of 1200 r/min, FSW only resulted in significant refinement of the W-phase and did not change the phase composition in the NZ.

Figure 6 shows the SEM images of the PM and NZ at different rotation rates. The W-phase particles are quite coarse (maximum particle size is ~10 μm) and the distribution is very heterogeneous in the PM (Fig. 6(a)). In the NZ, significantly refined W-phase particles are homogeneously distributed in the magnesium matrix, and the average particle size decreases clearly with increasing rotation rate (Fig. 6(b)–(d)). The average particle size is 3.2, 2.1 and 1.3 μm for 600, 800 and 1200 r/min, respectively. This is because the threaded pin has significant breaking and dispersion action on the W-phase particles in the NZ during FSW, and this action is enhanced with increasing rotation rate. The fine and dispersed W-phase particle would significantly restrain the growth of recrystallized grain in the NZ due to the pinning effect (Fig. 2(b)–(d)).

There are two competitive factors influencing the recrystallized grain size in the NZ, *i.e.* second phase particle and heat input. With increasing rotation rate, the increased heat input resulted in the growth of the recrystallized grains, whereas the dispersed fine W-phase particle produced by severer plastic deformation and stirring action significantly inhibited the growth of recrystallized grains. At the lower rotation rate of 600 r/min, the heat input should be the dominant factor determining the grain refinement, and therefore lower heat input resulted in significant refinement of the recrystallized grains. As the rotation rate increased, however, particle refinement gradually became the dominant factor. Thus, fine grains could be still obtained even at 1200 r/min because the growth of recrystallized grains was restrained. In the previous work[22], it was reported that the existence of a high volume fraction of the second phase resulted in inhomogeneous plastic deformation during FSW brass and inhibited DRX, producing the partial recrystallization zone in the NZ. These results indicated that the existence of second phase particles had a significant effect on the DRX in the NZ during FSW.

Figure 7 shows the hardness profiles along the mid-thickness of the plate on the cross-section of the welds at different rotation rates. The FSW welds at three rotation rates exhibit the similar hardness profiles. The hardness values within the NZ are higher than that of the PM, which is attributed to the reduced recrystallized grain size and the fine dispersed ternary eutectic phase particles (W-phase) in the NZ (Figs. 2(b)–(d) and 6(b)–(d)). Similarly, in FSW heat-proof

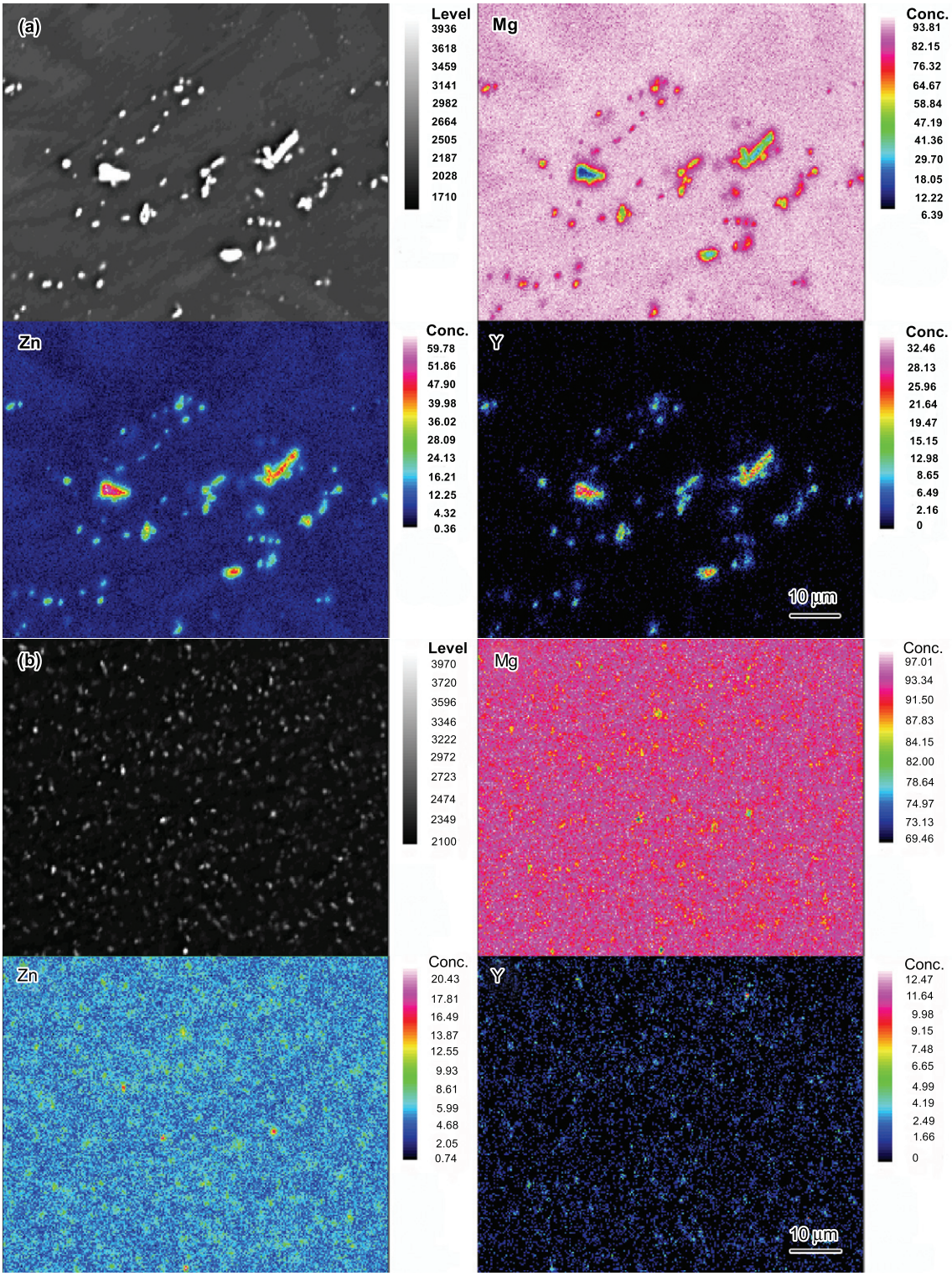

Fig. 5 Map distributions of Mg, Zn and Y elements by EPMA: (a) PM, (b) NZ of FSW Mg–Zn–Y–Zr joint at 1200 r/min–100 mm/min

Mg–Al–Ca alloy, it was reported that the hardness values in the NZ were higher than that in the PM due to the refined grains and porphyrization of the initial bulky secondary phase[20].

At the rotation rate of 600 r/min, the NZ exhibits the highest hardness values due to the finest recrystallized grains at the low heat input. Though similar grain sizes are obtained, the hardness of the NZ at 1200 r/min is slightly higher than that of the NZ at 800 r/min, and this should be attributed to the strengthening effect of the finer W-phase particles. Therefore, the recrystallized grain size and second phase particle size exhibit significant effect on the hardness of the NZ. With increasing rotation rate,

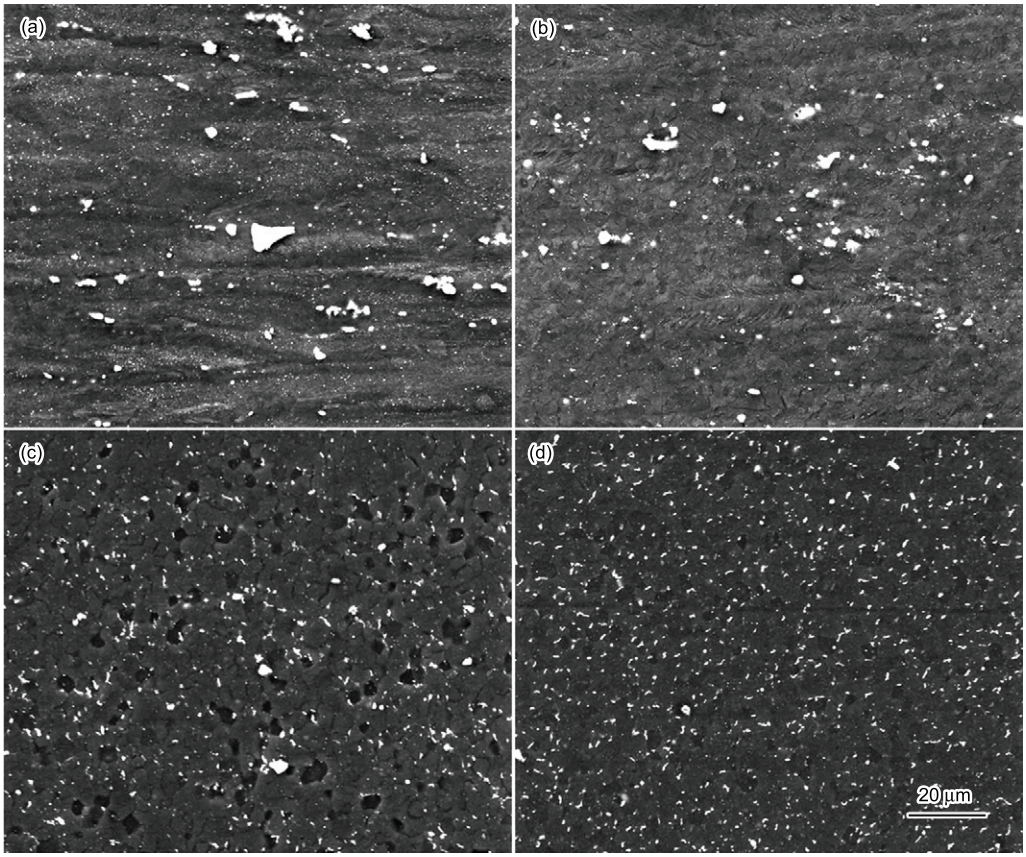

Fig. 6 SEM images of PM (a) and NZ of FSW Mg–Zn–Y–Zr joints at 600 (b), 800 (c) and 1200 r/min (d) with a traverse speed of 100 mm/min

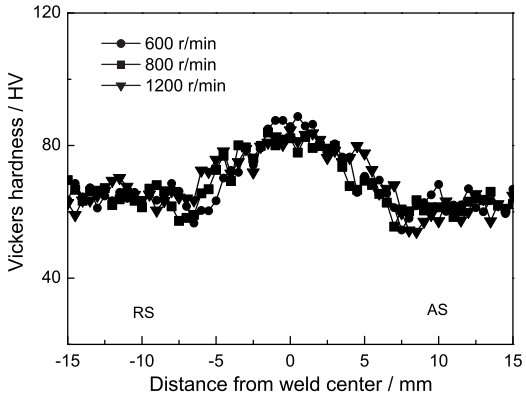

Fig. 7 Hardness profiles in cross sections of welds at various rotation rates (RS and AS are retreating side and advancing side, respectively)

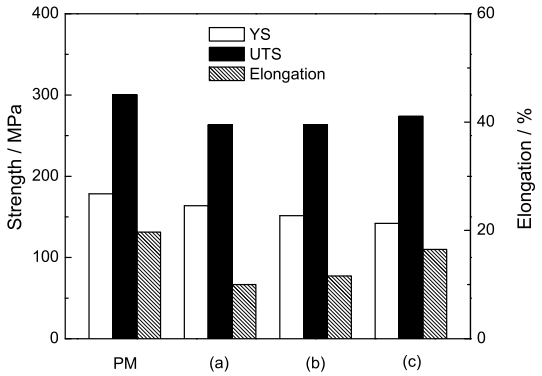

Fig. 8 Transverse tensile properties of PM and FSW joints at 600 (a), 800 (b) and 1200 r/min (c) (traverse speed: 100 mm/min)

i.e. increasing heat input, the high hardness zone is widened (Fig. 7), which is due to enhanced material flow at higher rotation rate.

Similar to the FSW Mg–Zn–Y–Zr alloy containing I-phase[18], the lowest hardness values of the welds at various rotation rates were observed in the HAZ, and the hardness value of the HAZ was very close to that of the PM. The reduction of the hardness in HAZ is attributed to the slightly annealing softening of rolled Mg–Zn–Y–Zr plate during FSW thermal cycle.

The transverse tensile properties of the FSW joints are shown in Fig. 8. Compared to the PM, the FSW joints exhibit decreased ultimate tensile strength (UTS), yield strength (YS) and elongation. With increasing rotation rate, the YS and YS/UTS of the FSW joints somewhat decrease, but the elongation remarkablely increases. Similarly, increasing rotation rate led to the increased elongation of FSW ZK60 alloy joints[17]. It is attributed to increased heat

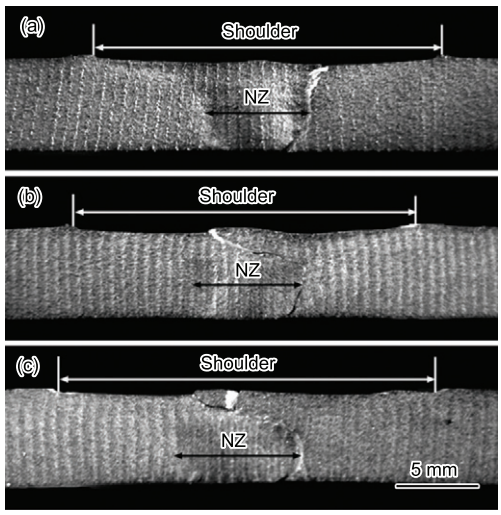

Fig. 9 Failed FSW Mg–Zn–Y–Zr joints at 600 (a), 800 (b) and 1200 r/min (c) (traverse speed: 100 mm/min; the advancing side is on the right side)

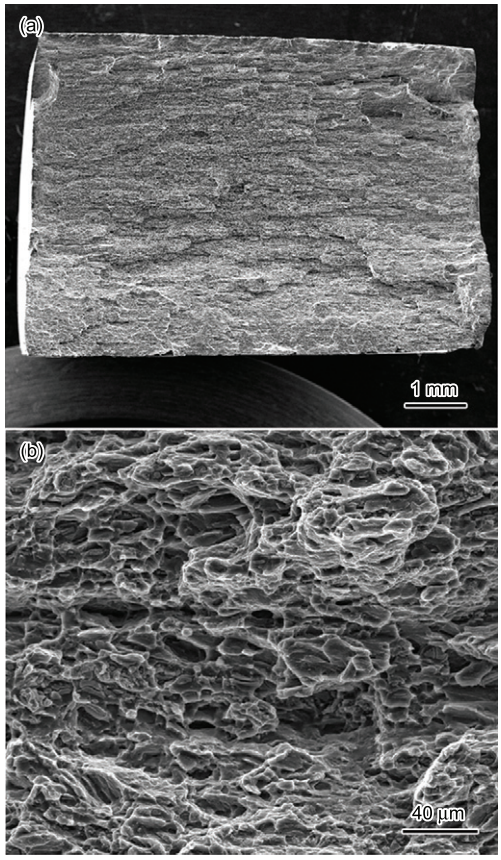

Fig. 10 SEM images showing fracture surface of welded joint at 600 r/min–100 mm/min

input resulting in the softening zone under thermal cycle of FSW. In this study, the UTS of FSW joints is similar and approaches to ∼90% of that of the PM.

Figure 9 shows the failed FSW Mg–Zn–Y–Zr alloy joints. For all the joints, the fracture occurs in the TMAZ of the advancing side, where plastic deformation is observed. The SEM micrographs of the fracture surface of the welded joint at 600 r/min are shown in Fig. 10. The fracture surfaces consist of tear ridges, dimples and cleavage facets, showing the characteristic of the plastic deformation. Similarly, compared to the welded joint at 600 r/min, the welded joints at 800 and 1200 r/min exhibit obviously plastic deformation due to the higher elongation. It indicates that the weakest region is located in the TMAZ, rather than the HAZ with the lowest hardness values. This implies that the hardness is not the only factor in determining the strength of the FSW magnesium alloys. The tensile properties of the FSW joints would probably be governed by the texture.

Significantly different orientations of the grains and W-phase particles in the TMAZ and NZ under different rotation rate were observed. Woo *et al.*[23] reported that the fracture location of friction stir processed AZ31 alloy was close to the boundary between the transition zone (*i.e.*, TMAZ) and NZ on the advancing side due to significant texture variation resulting from the incompatibility of the plastic deformation. Therefore, the different orientations of grains and second phase particles between the NZ and TMAZ should be the dominant factor in determining the mechanical properties of the FSW Mg–Zn–Y–Zr joints. Increasing the rotation rate resulted in the grain coarsening in the TMAZ, thus the reduced yield strength and enhanced elongation were obtained.

4. Conclusions

(1) Under a wide rotation rate range of 600–1200 r/min and a traverse speed of 100 mm/min, rolled Mg–Zn–Y–Zr alloy plates with 6 mm in thickness were successfully friction stir welded.

(2) The sizes of both grains and W-phase particles in the NZ were significantly refined compared to that in the PM. As the rotation rate increased the grain size increased, whereas the size of W-phase particles decreased. The TMAZ exhibited elongated deformed grains with coarse W-phase particle being distributed along flow lines.

(3) Under different rotation rates, the hardness values of the NZ were higher than that of the PM. At 600 r/min, the hardness values of the NZ were higher than those of NZs at 800 and 1200 r/min, due to finest recrystallized grain size. The lowest hardness values occurred at the HAZ, and the hardness was close to that of the PM.

(4) The UTS, YS and elongation of the FSW joints at various rotation rates were slightly lower than those of the PM, and the joints efficiency was as high as 90%. With increasing rotation rate, the UTS was similar and YS somewhat decreased, but the elongation increased clearly. The fracture occurred in the TMAZ for all the FSW Mg–Zn–Y–Zr joints.

Acknowledgement

This work was supported by the National Natural Sci-

ence Foundation of China (No. 51001023).

REFERENCES

[1] I.J. Polmear: *Light Alloys*, 3rd edn, London, 1995.
[2] M.M. Avedesian and H. Baker: *Magnesium and Magnesium Alloys*, ASM, USA, 1999.
[3] D.K. Xu, L. Liu, Y.B. Xu and E.H. Han: *Mater. Sci. Eng. A*, 2006, **420**, 322.
[4] W.M. Thomas, E.D. Nicholas, J.C. Needham, M.G. Murch, P. Templesmith and C.J. Dawes: G. B. Patent, No. 9125978. 8, 1991.
[5] R.S. Mishra and Z.Y. Ma: *Mater. Sci. Eng. R*, 2005, **50**, 1.
[6] K.S. Arora, S. Pandey, R. Kumar and M. Schaper: *J. Mater. Sci. Technol.*, 2010, **26**, 747.
[7] M. Jayaraman, R. Sivasubramanian and V. Balasubramanian: *J. Mater. Sci. Technol.* 2009, **25**, 655.
[8] J. Yang, B.L. Xiao, D. Wang and Z.Y. Ma: *Mater. Sci. Eng. A*, 2010, **527**, 708.
[9] X. Cao and M. Jahazi: *Mater. Des.*, 2009, **30**, 2033.
[10] M.A. Gharacheh, A.H. Kokabi, G.H. Daneshi, B. Shalchi and R. Sarrafi: *Int. J. Mach. Tool. Manu.*, 2006, **46**, 1983.
[11] S.H.C. Park, Y.S. Sato and H. Kokawa: *Scripta Mater.*, 2003, **49**, 161.
[12] A.R. Rose, K. Manisekar and V. Balasubramanian: *J. Mater. Eng. Perform.,* doi: 10.1007/s11665-011-9889-0.
[13] W.B. Lee, Y.M. Yeon and S.B. Jung: *Mater. Sci. Technol.*, 2003, **19**, 785.
[14] S.H.C. Park, Y.S. Sato and H. Kokawa: *J. Mater. Sci.*, 2003, **38**, 4379.
[15] J.A. Esparza, W.C. Davis and L.E. Murr: *J. Mater. Sci.*, 2003, **38**, 941.
[16] G.M. Xie, Z.Y. Ma and L. Geng: *Mater. Sci. Eng. A*, 2008, **486**, 49.
[17] G.M. Xie, L. Geng and Z.Y. Ma: *Acta Metall. Sin.*, 2008, **44**, 119. (in Chinese)
[18] G.M. Xie, Z.Y. Ma, L. Geng and R.S. Chen: *Mater. Sci. Eng. A*, 2007, **471**, 63.
[19] G.M. Xie, Z.Y. Ma and L. Geng: *J. Mater. Sci. Technol.*, 2009, **25**, 351.
[20] D.T. Zhang, S. Mayumi and M. Kouichi: *Scripta Mater.*, 2005, **52**, 899.
[21] S.E. Ion, F.J. Humpherys and S.H. White: *Acta Metall.*, 1982, **30**, 1909.
[22] G.M. Xie, Z.Y. Ma and L. Geng: *Philos. Mag.*, 2009, **89**, 1505.
[23] W. Woo, H. Choo, D.W. Brown, P.K. Liaw and Z. Feng: *Scripta Mater.*, 2006, **54**, 1859.